JSTR
ASEAN Journal of Scientific and Technological Reports

Research article

Experimental Study on Convective Heat Transfer and Pressure Drop Characteristics of an Alternating Cross-Section Flattened Tube with Different Twist Angle

Kunlakarn Warnropru[1], Jatuporn Kaew-On[2] and Nares Chimres[3*]

[1] Energy Engineering Program, Faculty of Engineering, Thaksin University, Phatthalung, 93210, Thailand; kunlakarn.fah@gmail.com
[2] Mechanical Engineering Program, Faculty of Engineering, Thaksin University, Phatthalung, 93210, Thailand; kaew_on@yahoo.com
[3] Mechanical Engineering Program, Faculty of Engineering, Thaksin University, Phatthalung, 93210, Thailand; nares_ch@yahoo.com
* Correspondence: nares_ch@yahoo.com

Citation:
Warnropru, K.; Kaew-On, J.; Chimres, N. Experimental Study on Convective Heat Transfer and Pressure Drop Characteristics of an Alternating Cross-Section Flattened Tube with Different Twist Angle. *ASEAN J. Sci. Tech. Report.* **2023**, *26*(1), 40-51. https://. 10.55164/ajstr.v26i1.248061

Article history:
Received: December 31, 2022
Revised: February 7, 2023
Accepted: February 10, 2023
Available online: March 21, 2023

Abstract: In this research, the heat transfer coefficient (HTC) and pressure drop of alternating cross-section flattened (ACF) tubes were investigated experimentally and compared with the same parameters of a circular tube. Three different ACF tubes were fabricated from circular copper tubing with an internal diameter of 4.5 mm, a thickness of 1 mm, and a length of 400 mm. The twist angles were 30, 45, and 90°. The experimental ranges covered a mass flux of 729–1,434 kg/m^{2}s and a heat flux of 12–30 kW/m^2. The results showed that the HTC and pressure drop increased with mass flux. The HTC decreased with increments of heat flux, but the pressure drop did not change. The HTC and pressure drop of the ACF tubes were higher than those of the circular tube. The ACF tube with 90° twist angles produced the highest HTC, and the thermal performance of that tube was about 27% better than the thermal performance of the circular tube.

Keywords: Alternating Cross-section Flattened (ACF) Tube; Heat Transfer Coefficient (HTC); Pressure Drop; Single-phase Heat Transfer

1. Introduction

Heat exchangers are widely used in industrial and household applications. They can be found in refrigerating systems, air-conditioning systems in power plants, electronic cooling systems, air-conditioners, and water heaters. Therefore, improvements in the thermal performances of heat exchangers can provide widespread benefits. Methods of increasing heat transfer can be divided into three categories: active, passive, and compound techniques [1]. The passive technique is generally preferred because this method does not need any external energy to enhance heat transfer. The objective can be achieved by inserting twinned coil/twisted tape into the tube [2-6], adding nanoparticles to the base fluid [7-11], and modifying the tube structure of the heat exchanger, such as with a corrugated tube [12-14], a micro-fin tube [15-16], a flattened tube [17-18], a twisted flattened tube [19], or a twisted oval tube [20-21]. These reports concluded that modifying the tube shape to enhance the heat transfer of the internal flow was an attractive approach.

In 2020, Sajadi and Talebi [22] investigated the convective heat transfer, pressure drop, and efficiency of ZnO/water nanofluid flowing in alternating elliptical axis (AEA) tubes in a Reynolds number (Re) range of 400 to 1,900. The rotation angle of the AEA was 90° along the tube length. They found that

increasing the tube flattening increased the heat transfer rate. The heat transfer and pressure drop of the AEA tube were greater than that of a circular tube. In addition, a tube with medium flattening was the most efficient among the tested tubes. In 2022, they investigated the heat transfer and pressure drop of alternating flattened (AF) tubes filled with a TiO_2/oil nanofluid. Experiments were conducted on three different AF tubes with oil as the base fluid carrying TiO_2 nanoparticles at 1% and 2% volumetric concentrations between 400 and 1,800 Re. They reported that the heat transfer and pressure drop of the AF tubes were higher than those of a circular tube. Flattening the tube affected heat transfer and pressure drop, which were enhanced by increasing the concentration of TiO_2 nanoparticles [23].

Luo and Song [24] investigated the thermal performance enhancement of a double-tube heat exchanger with twisted annulus formed by counter-twisted oval tubes. The studied twisted oval tubes were configured with aspect ratios of 0.4, 0.5, and 0.6, and thermal performances were compared with the performances of conventional oval tubes. They found that the Nusselt number (Nu) and friction factor (f) increased by up to 157% and 118%, respectively.

Farsi et al. [25] examined the heat transfer and flow characteristics of an AF tube with a 90° twist angle. The factors of interest were straight pitch (a), transient length (b), and minimum axis (c). The numerical study focused on the laminar flow conditions within a Re range from 500 to 1,500. They found that the minimum axis produced the largest effects, followed by the transient length and straight pitch. The model tube with a = 10, b = 5, and c = 5.5 mm produced the best thermal performance factor of 2.27. Furthermore, Babaei et al. [26] conducted an experiment that simulated solar pond conditions. They evaluated the performance of serpentine AF coils with the same geometric factors (a), (b), and (c) as [25]. The results found that the deeply flattened (c) had the most effect, followed by (b) and (a), respectively.

Rukruang et al. [27] studied the heat transfer coefficient (HTC) and pressure drop of water flowing through a 90° alternating cross-section flattened (ACF) tube compared with a circular tube. The result showed that the HTC and flow resistance of the ACF tube were higher, and the thermal performance was 3.4 times better. Moreover, vortices were produced at the curved wall of the ACF tube and intensified in the flow direction. They reported that an alternating cross-section tube produced secondary flow and turbulence intensity through the tube curvature. Multi-longitudinal vortices formed along the length of the tube, which produced a significant enhancement in the heat transfer performance of the tube [28]. Furthermore, their study investigated the air-side performance of ACF tube heat exchangers with three hydraulic diameters of 4.16, 4.75, and 5.20 mm. All the ACF tube heat exchangers produced better heat transfer than circular tube heat exchangers. The 5.20 mm ACF tube provided the best heat transfer rate and pressure drop [29].

These previous studies have shown that flattening the tube increases the convective heat transfer potential of fluid near the tube wall by creating secondary flows and by increasing the turbulence of the flow. The characteristics of an ACF tube's cross-section area generate vortices and improve the mixing of fluids inside the tube. However, the pressure drop is also increased. Therefore, the heat transfer and the pressure drop of ACF tubes must be studied to improve thermal performance. Moreover, the effect of the twist angle of the ACF tube on heat transfer is very interesting, but little has been published about it.

2. Methodology

2.1 Experimental apparatus

The experimental study determined the HTC and pressure drop of single-phase water flowing inside ACF tubes with twist angles of 30° (ACF-30), 45° (ACF-45), and 90° (ACF-90). The ACF tubes were formed by pressing a circular copper tube with an internal diameter of 4.5 mm, a thickness of 1 mm, and a length of 400 mm (Fig. 1). The main components of the experimental apparatus consisted of a test section, a hot-water loop, a cold-water loop, a control panel, and a data acquisition system (Fig. 2). The detailed configurations of the ACF tubes are presented in Fig. 3(a-c).

Figure 1. The circular and alternating cross-section flattened (ACF) tubes

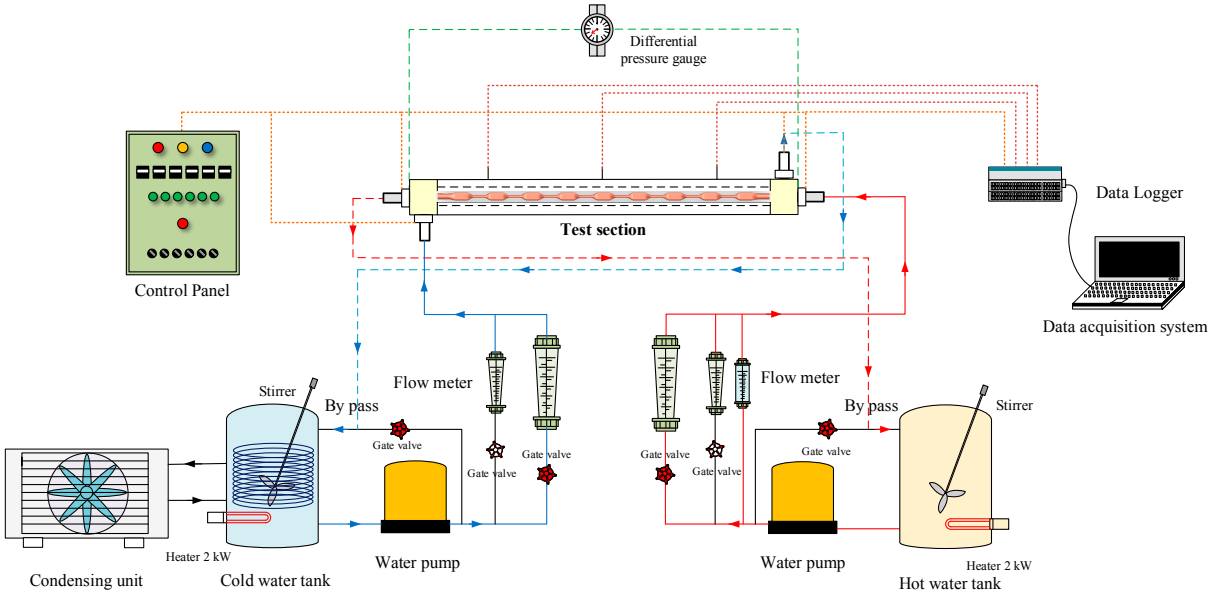

Figure 2. Schematic diagram of the experimental apparatus

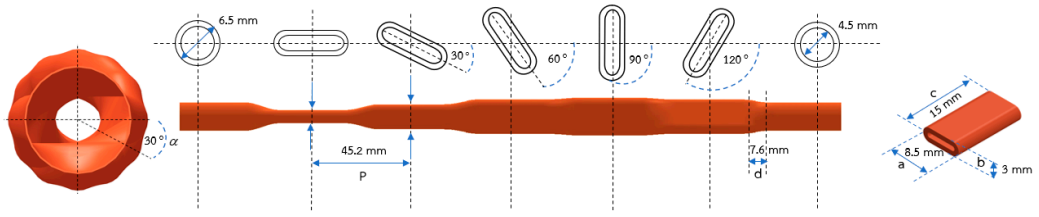

(a)

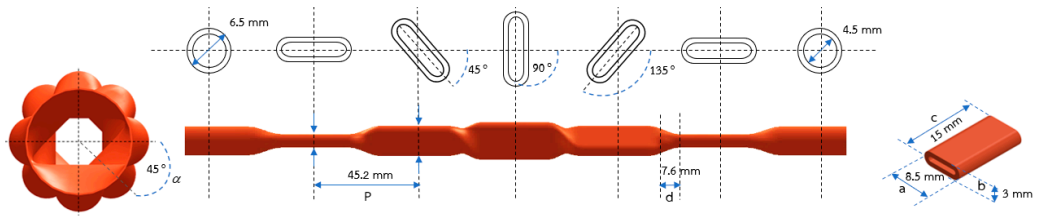

(b)

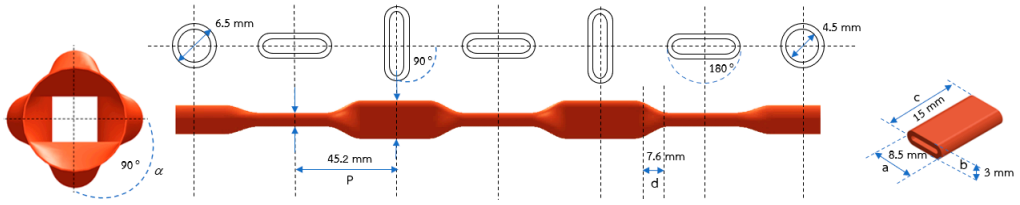

(c)

Figure 3. Configurations of alternating cross-section flattened tubes with twist angles of 30 ° (ACF-30) (a), 45° (ACF-45) (b), and 90° (ACF-90) (c)

The water in the hot-water loop was heated by an electrical heater and driven by a water pump through a flow meter to the inner tube of the test section. The hot water exchanged heat with the cold water flowing outside the ACF tube in the cold-water loop. A water pump drove the water in the cold-water loop through the shell in the test section. Seven thermocouples were installed: four at the headers and three along the wall of the ACF tube. A data logger collected all temperature measurements. The test section was a counterflow double-tube heat exchanger (Fig. 4). The outside of the test section was insulated with rubber insulation. The length between the two pressure taps was 400 mm, and a differential pressure gauge detected the pressure drop across the test section. The geometric configurations of the tested tubes and the test conditions are shown in Tables 1 and 2, respectively. Moreover, the direct measurement uncertainties and maximum experiment uncertainty are demonstrated in Table 3.

Table 1. Geometric configurations of the experimental tubes.

Tube Name	L (mm)	$D_{h,i}$ (mm)	a (mm)	b (mm)	c (mm)	d (mm)	P (mm)	α (degree)
Circular	400	4.50	-	-	-	-	-	-
ACF-30	400	1.96	8.50	3.00	15.00	7.60	45.20	30
ACF-45	400	2.05	8.50	3.00	15.00	7.60	45.20	45
ACF-90	400	2.18	8.50	3.00	15.00	7.60	45.20	90

Table 2. Test conditions.

Parameter	Operating conditions
Inlet water temperature $(^{\circ}C)$	30-40
Mass flux (kg/m²s)	729-1,434
Heat flux (kW/m²)	12-30

Table 3. Uncertainties of measurement devices and calculated parameters.

Parameter	Uncertainty
T-type thermocouple	$0.1\,^{\circ}C$
Flow meter of water	3% of full scale
Differential pressure gauge	1.6% of full scale
Heat transfer rate at test section $(\dot{Q}_{TS})$	14.87%
Heat transfer rate at preheater $(\dot{Q}_{PH})$	10.51%
Reynolds number (Re)	3.00%
Heat transfer coefficient (h_i)	9.82%
Nusselt number (Nu)	4.72%
Friction factor (f)	6.21%

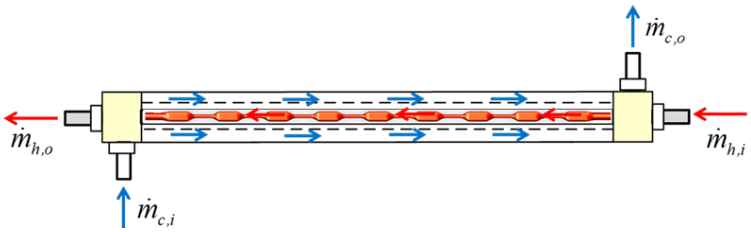

Figure 4. Diagram of the counterflow in the test section

2.2 Data Reduction

The data reduction of this experiment was classified into the following three categories.

2.2.1 Heat transfer

The heat transfer between the hot fluid and the cold fluid was calculated from

$$\dot{Q} = \dot{m}C_p(T_i - T_o) \tag{1}$$

where $\dot{Q}$ is the heat transfer rate, $\dot{m}$ is the mass flow rate of the fluid, T is the temperature of the fluid, and i and o are defined as the inlet and outlet of the test section, respectively.

The overall heat transfer coefficient was calculated as

$$U = \frac{\dot{Q}}{A \cdot LMTD} \tag{2}$$

where U is the overall heat transfer coefficient, A is the heat transfer area, and $LMTD$ is the log mean temperature difference.

The total thermal resistance of the ACF tube was determined from

$$\frac{1}{UA} = \frac{1}{h_o A_o} + \frac{1}{2\pi kL}\ln\left[\frac{D_{h,o}}{D_{h,i}}\right] + \frac{1}{h_i A_i} \tag{3}$$

where h_o is the heat transfer coefficient at the outside tube; A_i and A_o are the inner and outer surface area of the tube, respectively; k is the thermal conductivity of the tube; L is the total tube length, $D_{h,i}$ and $D_{h,o}$ are the inner and outer hydraulic diameter of the tube; h_i is inside heat transfer coefficient.

Since the ACF tube is a non-circular tube, the hydraulic diameter must be calculated. The hydraulic diameter was determined by

$$D_h = \frac{4A_{c,avg}}{p} \tag{4}$$

where $A_{c,avg}$ is the average cross-section area of the tube and p is the wetted perimeter of the tube.

2.2.2 Pressure drop

The total pressure drop (ΔP_{total}) is obtained from the sum of four pressure drop components as follows:

$$\Delta P_{total} = \Delta P_f + \Delta P_a + \Delta P_{cont} + \Delta P_{\exp} \tag{5}$$

Where ΔP_f is the frictional pressure drop, ΔP_a is the acceleration pressure drop, ΔP_{cont} is the sudden contraction pressure drop, and $\Delta P_{\exp}$ is the sudden enlargement pressure drop.

However, in the case of a single-phase horizontal flow such as the tested system, the acceleration pressure drop can be ignored. Moreover, the sudden contraction and sudden enlargement pressure drop are

very small compared to the frictional pressure and thus were not considered in this study. Therefore, the total pressure drop was represented as

$$\Delta P_{total} = \Delta P_f \tag{6}$$

The pressure drop of flow in the tube was determined by using the Darcy-Weisbach equation,

$$\Delta P = f \frac{L}{D_h} \rho \frac{v^2}{2} \tag{7}$$

where ΔP is the pressure drop, f is the Darcy friction factor, L is the tube length, D_h is the hydraulic diameter of the tube, ρ is the density of the fluid, and v is the average velocity.

The friction factors (f) were expressed as the calculated frictional pressure drop (ΔP_f) as

$$f = \frac{2D_{h,i}\Delta P}{L\rho v^2} \tag{8}$$

2.2.3 Thermal enhancement factor

Thermal enhancement factors (TEF) were calculated as the ratio between the Nusselt number and the friction factor of each ACF tube and the circular tube [30-31], using the following equation:

$$TEF = \frac{Nu_{ACF} / Nu_{cir}}{(f_{ACF} / f_{cir})^{1/3}} \tag{9}$$

Where Nu_{cir} and f_{cir} are respectively the Nusselt number and friction factor of the circular tube, and Nu_{ACF} and f_{ACF} are respectively the Nusselt number and friction factor of the ACF tube.

3. Results and Discussion

3.1 Validation of the experimental apparatus

The experimental apparatus was validated by comparing the experimental results with existing correlations. The selected parameters were the HTC and the frictional pressure drop of water flowing through the circular tube. The HTCs obtained in this experiment were compared with the correlations of Dittus-Boelter (1930), Colburn (1933), Petukhov (1970), and Gnielinski (1976). The frictional pressure drops obtained compared with the correlations of Moody (1947), Altshul (1952), Petukhov (1970), Churchil (1973), and Haaland (1983).

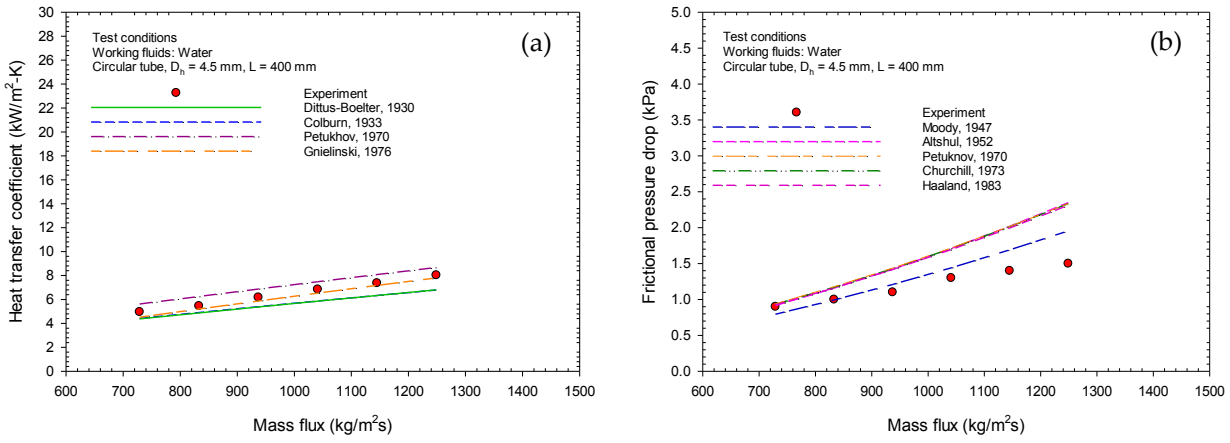

Figure 5. Comparison with existing correlations of the effect of mass flux on (a) the heat transfer coefficient and (b) the frictional pressure drop in the present study

It was found that when the mass flux was increased, the HTC and the pressure drop from friction increased. The experimental HTCs were similar to the HTCs obtained by Gnielinski (1976), with an average error of 4.77% (Fig. 5). The experimental frictional pressure drops were lower than those obtained in the previous works, but the trend of change was similar. The experimental results were closest to those of Moody (1947), with an average error of 14.02%.

3.2 Effect of heat flux on the HTC and pressure drop

The effects of heat flux on HTC and pressure drop were investigated for the ACF and circular tubes. The inlet water temperature (IWT) was fixed at 35 °C . The mass flux range was 800-900 kg/m²s. The four different heat fluxes in this investigation were 13, 17, 21, and 25 kW/m².

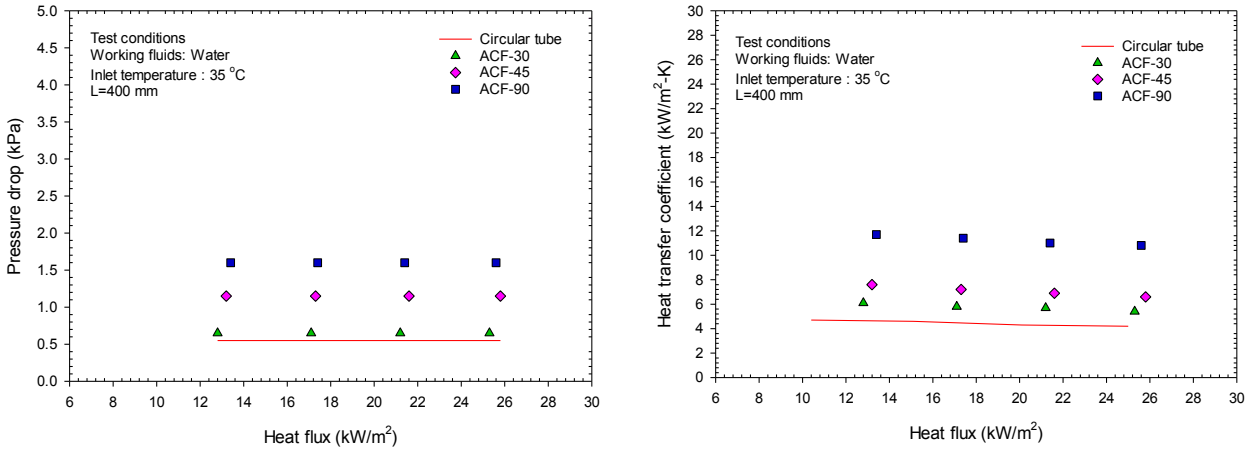

(a) (b)

Figure 6. Effect of heat flux on (a) the pressure drop and (b) the heat transfer coefficient in a circular tube and alternating cross-section flattened tubes with twist angles of 30° (ACF-30), 45° (ACF-45) and 90° (ACF-90)

Increases in heat flux did not affect the pressure drop. The pressure drop was larger in all the ACF tubes than in the circular tube (Fig. 6(a)). The largest pressure drop was observed in the ACF-90, followed by the ACF-45 and ACF-30. The mean pressure drop of the ACF-90 was about 190.91% higher than that of the circular tube. The mean pressure drops of the ACF-45 and ACF-30 were 109.09% and 18.18% higher than the mean pressure drop of the circular tube. Regarding the twist angle, the ACF-90 provided the best HTC because the change in the internal cross-section area of the ACF-90 was more sudden. The change in the cross-section area of the ACF-45 was less than the change in the ACF-90 but greater than the ACF-30 (Fig. 7). The different tube structures caused different pressure drops. The change in pressure drop is greater when the change in the cross-sectional area of the tube is greater. Therefore, the ACF-90 gave the largest pressure drop, followed by the ACF-45 and ACF-30, respectively. The pressure drop in the circular tube was the lowest because the cross-sectional area of a circular tube is constant.

Increases in heat flux resulted in slight decreases in the HTC. All three ACF tubes gave a higher HTC than the circular tube (Fig. 6(b)). The ACF-90 provided the highest HTC, followed by the ACF-45 and ACF-30. The average HTC of the ACF-90 was about 152.43% higher than that of the circular tube. The average HTCs of the ACF-45 and ACF-30 was 58.72% and 28.91% higher than the average HTC of the circular tube, respectively. The fluid flowing in the outer tube could not absorb the heat so efficiently from the surface of the circular inner tube because the hottest fluid, in the mainstream at the center of the inner tube, was far from the tube surface. In the ACF tubes, the flow of fluid was different. The flattened shape of the inner tube brought the hottest fluid closer to the inner tube surface, so the colder fluid in the outer tube could absorb the heat of the fluid in the ACF tubes better than the heat of the fluid flowing in the circular tube.

Since the variation in the change of the cross-section area of the ACF-90 is very high, the turbulence of the heated fluid is increased more. The turbulence of the heated fluid in the inner tube directly affects the HTC; therefore, the HTC produced by the ACF-90 was highest, followed by the HTC produced by the ACF-45, the ACF-30, and finally, the circular tube.

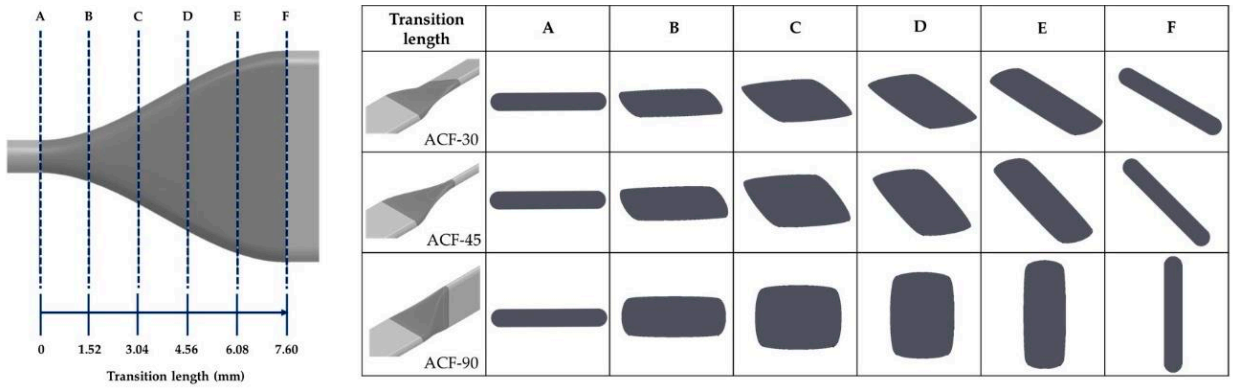

Figure 7. The cross-section area variation in the transition region of the alternating cross-section flattened (ACF) tubes

3.3 Effect of mass flux on the HTC and pressure drop

The effects of mass flux were investigated on the HTC and pressure drop. The mass flux affected both the HTC and pressure drop. The HTC and pressure drop increased when the mass flux increased (Fig. 8). The effects of the ACF tube twist angle on the HTC and pressure drop at different mass fluxes showed the same tendency as the effect of twist angles at different heat fluxes. The mass flux range in this investigation was 729-1,434 kg/m^{2}s at an inlet temperature of 35 $^\circ$C , while the heat flux range was 12.7-15.2 kW/m^2.

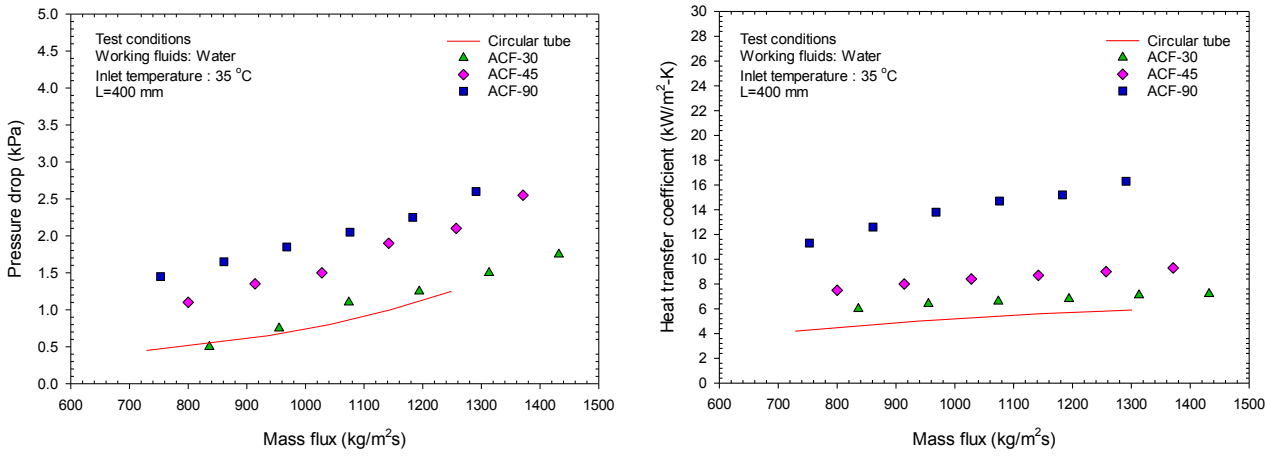

(a) (b)

Figure 8. Effect of mass flux on (a) the pressure drop and (b) the heat transfer coefficient of a circular tube and alternating cross-section flattened tubes with twist angles of 30° (ACF-30), 45° (ACF-45), and 90° (ACF-90)

3.4 Effect of the inlet water temperature on the HTC and pressure drop

The inlet water temperature (IWT) effects on the HTC and pressure drop were investigated (Fig. 9). The IWTs in this study were 30, 35, and 40 $^\circ$C under 17 kW/m^2 of heat flux and 800 kg/m^{2}s of mass flux.

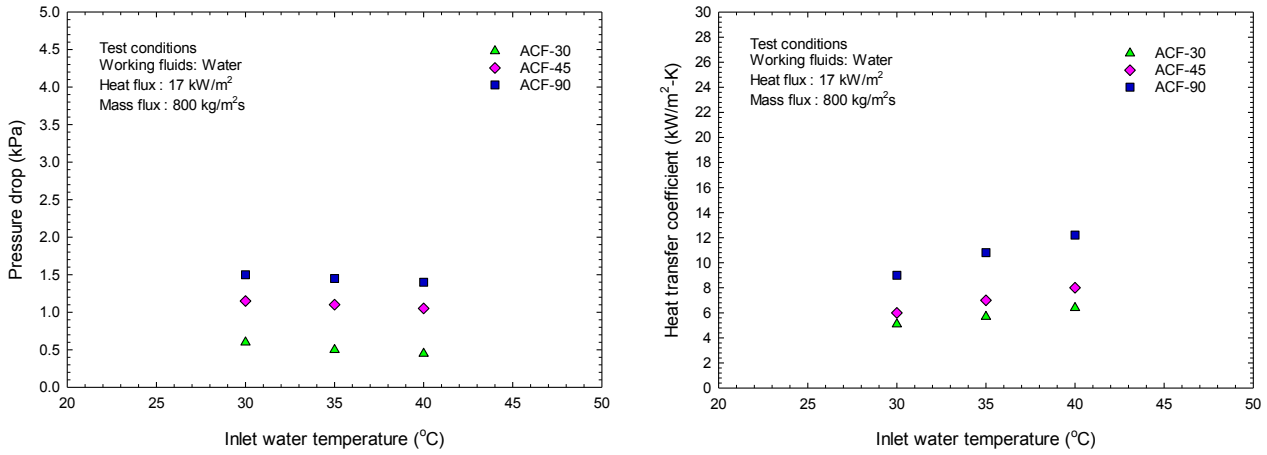

Figure 9. Effect of the inlet water temperature on (a) the pressure drop and (b) the HTC of a alternating cross-section flattened tubes with twist angles of 30° (ACF-30), 45° (ACF-45), and 90° (ACF-90)

The IWT affected the HTC and pressure drop, but the change trends differed. The HTC increased when the IWT increased, but the pressure drop decreased when the IWT increased (Fig. 9). Some thermal properties of water vary with the water temperature. The thermal conductivity of water increases when the temperature increases, which mainly affects the HTC. On the other hand, as the temperature of water increases, its viscosity decreases, which causes the pressure drop to decrease as the IWT increases.

3.5 Performance index comparison

The performance index (PI) was determined by the TEF. The TEF as a function of the Re is shown for each tube in Fig. 10.

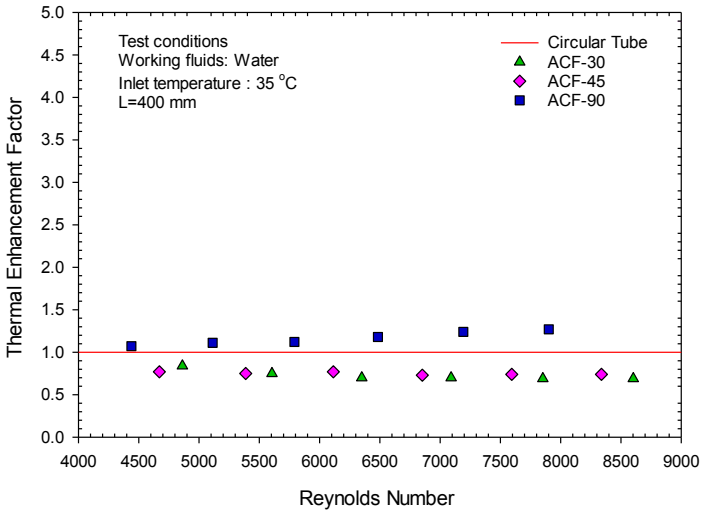

Figure 10. The TEF with Reynolds numbers of each tube

The results show that only the ACF-90 gave a higher TEF than the circular tube. The other ACF tubes produced lower TEFs than the circular tube. Although the HTCs of the ACF-45 and ACF-30 were higher than the HTC of the circular tube, the increases in friction factors were greater. As a result, the TEFs of these ACF tubes were lower than the TEF of the circular tube. The ACF-90 produced a TEF of 1.27, which was 27% larger than the TEF of the circular tube.

4. Conclusions

The flow and heat transfer characteristics of water flowing through alternating cross-section flattened (ACF) tubes were studied. The effects of the twist angle of ACF on heat transfer and pressure drop were also investigated. The thermal performances of three different ACF tubes were compared with the thermal performance of a circular tube. The following conclusions are presented.

- The HTC and pressure drop produced by the most effective ACF exceeded the HTC and pressure drop of the circular tube by approximately 28.91%-152.43% and 18.18%-190.91%, respectively.

- The ACF tube with a twist angle of 90 degrees produced the highest HTC and pressure drop. Compared with the circular tube, the HTC and pressure drop increased by 152.43% and 190.91%.

- The thermal enhancement factor (TEF) of the ACF tube was about 27% higher than the TEF of the circular tube. Therefore, alternating cross-section flattened tubes are suitable replacements for circular tubes in heat exchangers.

5. Acknowledgements

This work was supported by the Research and Development Intitute, Thaksin University (RDITSU)'s Research Fund, grant number 10-01/2563.

Author Contributions: Kunlakarn Warnropru carried out the experimental results, interpreted the results, and aided in drafting the manuscript. Nares Chimres and Jatuporn Kaew-On participated in designing the study and analysis and gave final proof of the manuscript.

Funding: The Research and Development Intitute, Thaksin University (RDITSU)'s Research Fund, grant number 10-01/2563.

Conflicts of Interest: The authors declare that there is no conflict of interest regarding the publication of this article.

References

[1] Webb, R.L.; Kim, N.H. *Principles Enhanced Heat Trans*, 2nd ed.; Taylor & Francis Group: 270 Madison Avenue, New York, 2005, 3-10. https://doi.org/10.1201/b12413

[2] Dang, W.; Wang, L.B. Convective heat transfer enhancement mechanisms in circular tube inserted with a type of twined coil. *Int. J. Heat Mass Transf.* 2021, *169*, 120960. https://doi.org/10.1016/j.ijheatmasstransfer.2021.120960

[3] Cong, T.; Wang, B.; Gu, H. Numerical analysis on heat transfer enhancement of sCO_2 in the tube with twisted tape. *Nucl. Eng. Des.* 2022, *397*, 111940. https://doi.org/10.1016/j.nucengdes.2022.111940

[4] Harish, H.V.; M-Tech.; Manjunath, K. Heat and fluid flow behaviors in a laminar tube flow with circular protruded twisted tape inserts. *Case Stud. Therm. Eng.* 2022, *32*, 101880. https://doi.org/10.1016/j.csite.2022.101880

[5] Kaood, A.; Fadodun, O.G. Numerical investigation of turbulent entropy production rate in conical tubes fitted with a twisted-tape insert. *Int. Commun. Heat Mass Transf.* 2022, *139*, 106520. https://doi.org/10.1016/j.icheatmasstransfer.2022.106520

[6] Zhang, H.; Nunayon, S.S.; Jin, X.; Lai, A.C.K. Pressure drop and nanoparticle deposition characteristics for multiple twisted tape inserts with partitions in turbulent duct flows. *Int. J. Heat Mass Transf.* 2022, *193*, 121474. https://doi.org/10.1016/j.ijheatmasstransfer.2021.121474

[7] Pourpasha, H.; Heris, S.Z.; Mahian, O.; Wongwises, S. The effect of multi-wall carbon nanotubes/turbine meter oil nanofluid concentration on the thermophysical properties of lubricants. *Powder Technology.* 2020, *367*, 133-142. https://doi.org/10.1016/j.powtec.2020.03.037

[8] Ho, C.J.; Huang, S.H.; Lai, C.M. Enhancing laminar forced convection heat transfer by using Al_2O_3/PCM nanofluids in a concentric double-tube duct. *Case Stud. Therm. Eng.* 2022, *35*, 102147. https://doi.org/10.1016/j.csite.2022.102147

[9] Ozenbiner, O.; Yurddas, A. Numerical analysis of heat transfer of a nanofluid counterflow heat exchanger. *Int. Commun. Heat Mass Transf.* 2022, *137*, 106306. https://doi.org/10.1016/j.icheatmasstransfer.2022.106306

[10] Zhang, C.; Han, S.; Wu, Y.; Zhang, C.; Guo, H. Investigation on convection heat transfer performance of quaternary mixed molten salt based nanofluids in smooth tube. *Int. J. Therm. Sci.* 2022, *177*, 107534. https://doi.org/10.1016/j.ijthermalsci.2022.107534

[11] Ma, H.; He, B.; Su, L.; He, D. Heat transfer enhancement of nanofluid flow at the entry region of microtubes. *Int. J. Therm. Sci*. 2023, *184*, 107944. https://doi.org/10.1016/j.ijthermalsci.2022.107944

[12] Cruz, G.G.; Mendes, M.A.A.; Pereira, J.M.C.; Santos, H.; Nikulin, A.; Moita, A.S. Experimental and numerical characterization of single-phase pressure drop and heat transfer enhancement in helical corrugated tubes. *Int. J. Heat Mass Transf.* 2021, *179*, 121632. https://doi.org/10.1016/j.ijheatmasstransfer.2021.121632

[13] Cheng, X.; Li, Z-R.; Wan, H-N.; Bi, Q.; Ji, W-T. Experimental investigation on convective heat transfer of hydrocarbon fuel in transverse corrugated tubes. *Int. J. Heat Mass Transf*. 2023, *201*, 123586. https://doi.org/10.1016/j.ijheatmasstransfer.2022.123586

[14] Liao, W.; Lian, S. Effect of compound corrugation on heat transfer performance of corrugated tube. *Int. J. Therm. Sci.* 2023, *185*, 108036. https://doi.org/10.1016/j.ijthermalsci.2022.108036

[15] Holagh, S.G.; Abdous, M.A.; Rastan, H.; Shafiee, M.; Hashemian, M. Performance analysis of micro-fin tubes compared to smooth tubes as a heat transfer enhancement technique for flow condensation. *Energy Nexus*. 2022, *8*, 100154. https://doi.org/10.1016/j.nexus.2022.100154

[16] Moon, S.H.; Lee, D.; Kim, M.; Kim, Y. Evaporation heat transfer coefficient and frictional pressure drop of R600a in a micro-fin tube at low mass fluxes and temperatures. *Int. J. Heat Mass Transf*. 2022, *190*, 122769. https://doi.org/10.1016/j.ijheatmasstransfer.2022.122769

[17] Kaew-On, J.; Naphattharanun, N.; Binmud, R.; Wongwises, S. Condensation heat transfer characteristics of R134a flowing inside mini circular and flattened tubes. *Int. J. Heat Mass Transf*. 2016, *102*, 86-97. http://dx.doi.org/10.1016/j.ijheatmasstransfer.2016.05.095

[18] Azarhazin, S.; Sajadi, B.; Fazelnia, H.; Behabadi, M.A.A.; Zakeralhoseini, S. Boiling heat transfer coefficient and pressure drop of R1234yf flow inside smooth flattened tubes: An experimental study. *Appl. Therm. Eng*. 2020, *165*, 114595. https://doi.org/10.1016/j.applthermaleng.2019.114595

[19] Razzaghi, M.J.P; Ghassabian, M.; Daemiashkezari, M.; Abdulfattah, A.N.; Afrouzi, H.H.; Ahmad, H. Thermo-hydraulic performance evaluation of turbulent flow and heat transfer in a twisted flat tube: A CFD approach. *Case Stud. Therm. Eng.* 2022, *35*, 102107. https://doi.org/10.1016/j.csite.2022.102107

[20] Liu, S.; Yin, Y.; Tu, A.; Zhu, D. Experimental investigation on shell-side performance of a novel shell and tube oil cooler with twisted oval tubes. *Int. J. Therm. Sci.* 2020, *152*, 106290. https://doi.org/10.1016/j.ijthermalsci.2020.106290

[21] Li, X.; Wang, L.; Feng, R.; Wang, Z.; Liu, S.; Zhu, D. Study on shell side heat transport enhancement of double tube heat exchangers by twisted oval tubes. *Int. Commun. Heat Mass Transf.* 2021, *124*, 105273. https://doi.org/10.1016/j.icheatmasstransfer.2021.105273

[22] Sajadi, A.; Talebi, S. Investigation of convective heat transfer, pressure drop and efficiency of ZnO/water nanofluid in alternating elliptical axis tubes. *Energy Equip. Sys.* 2020, *8*, 203-215. 10.22059/EES.2020.44634

[23] Sajadi, A.; Talebi, S. Experimental investigation of heat transfer, pressure drop, and efficiency of TiO_2/Oil nanofluid in alternating flattened tubes. *Energy Equip. Sys*. 2022, *10*, 123-136. https://doi.org/10.22059/EES.2022.253058

[24] Luo, C.; Song, K. Thermal performance enhancement of a double-tube heat exchanger with novel twisted annulus formed by counter-twisted oval tubes. *Int. J. Therm. Sci*. 2021, *164*, 106892. https://doi.org/10.1016/j.ijthermalsci.2021.106892

[25] Farsi, M.; Khoshvaght-Aliabadi, M.; Alimoradi, A. A parametric study on heat transfer and pressure drop characteristics of circular tube with alternating flattened flow path. *Int. J. Therm. Sci*. 2021, *160*, 106671. https://doi.org/10.1016/j.ijthermalsci.2020.106671

[26] Babaei, H.R.; Khoshvaght-Aliabadi, M.; Mazloumi, S.H. Analysis of serpentine coil with alternating flattened axis: An insight into performance enhancement of solar ponds. *Solar Energy*. 2021, *217*, 292-307. https://doi.org/10.1016/j.solener.2021.02.017

[27] Rukruang, A.; Chimres, N.; Kaew-On, J.; Wongwises, S. Experimental and numerical study on heat transfer and flow characteristics in an alternating cross-section flattened tube. *Heat Transf. Res*. 2019, *48*, 817-834. https://doi.org/10.1002/htj.21407

[28] Rukruang, A.; Chimres, N.; Kaew-On, J.; Mesgarpour, M.; Mahian, O.; Wongwises, S. A critical review on the thermal performance of alternating cross-section tubes. *Alexandria Eng. J.* 2022, *61*, 7315-7337. https://doi.org/10.1016/j.aej.2021.12.070

[29] Rukruang, A.; Chittiphalungsri, T.; Chimres, N.; Kaew-On, J.; Mesgarpour, M.; Mahian, O.; Wongwises, S. Experimental Investigation of Thermal Performance of a Novel Alternating Cross-Section Flattened Tube Heat Exchanger. *Int. J. Heat Mass Transf*. 2022, *195*, 123159. https://doi.org/10.1016/j.ijheatmasstransfer.2022.123159

[30] WEBB, R.L. Performance evaluation criteria for use of enhanced heat transfer surfaces in heat exchanger design. *Int. J. Heat Mass Transf*. 1981, *24*, 715-726. https://doi.org/10.1016/0017-9310(81)90015-6

[31] Skullong, S.; Promvonge, P.; Thianpong, C.; Jayranaiwachira, N. Thermal behaviors in a round tube equipped with quadruple perforated-delta-winglet pairs. *Appl. Therm. Eng*. 2017, *115*, 229-243. https://doi.org/10.1016/j.applthermaleng.2016.12.082